ACS APPLIED MATERIALS & INTERFACES

Letter

www.acsami.org

Development of Upconversion Luminescent Probe for Ratiometric Sensing and Bioimaging of Hydrogen Sulfide

Shujuan Liu,[†] Lili Zhang,[†] Tianshe Yang,[†] Huiran Yang,[†] Kenneth Yin Zhang,[†] Xin Zhao,[†] Wen Lv,[†] Qi Yu,[†] Xinglin Zhang,[†] Qiang Zhao,*[,†] Xiangmei Liu,[†] and Wei Huang*[,†,‡]

[†]Key Laboratory for Organic Electronics & Information Displays (KLOEID) and Institute of Advanced Materials (IAM), Nanjing University of Posts & Telecommunications (NUPT), 9 Wenyuan Road, Nanjing 210023, P. R. China

[‡]Institute of Advanced Materials (IAM) and Jiangsu-Singapore Joint Research Center for Organic/Bio- Electronics & Information Displays, Nanjing Tech University (NanjingTech), 30 South Puzhu Road, Nanjing 211816, P. R. China

Supporting Information

ABSTRACT: Merocyanines adsorbed into the mesopores of $mSiO_2$ shell of $NaYF_4$: 20% Yb, 2% Er, 0.2% Tm nanocrystals are demonstrated as ratiometric upconversion luminescence (UCL) probe for highly selective detection of HS^- in living cells through inhibition of energy transfer from the UCL of the nanocrystals to the absorbance of the merocyanines. The UCL probe has been used for ratiometric sensing of H_2S with high sensitivity and selectivity.

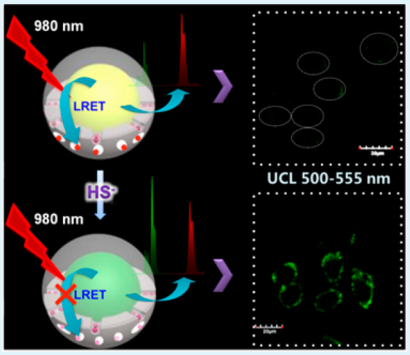

KEYWORDS: *hydrogen sulfide, lanthanoids, luminescence, nanoparticles, sensors*

Hydrogen sulfide (H_2S) has been considered as a notorious toxic gas for centuries because of its characteristic foul odor of rotten eggs and harmfulness to different systems in the body. Recent studies have established that H_2S is the third endogenously generated gaseous signaling compound (gasotransmitter) with cytoprotective properties besides nitric oxide (NO) and carbon monoxide (CO).[1] H_2S is involved in a wide range of physiological processes, including vasodilation,[2,3] angiogenesis,[4] apoptosis,[5] inflammation,[6] and neuromodulation, and an abnormal H_2S level is correlated to diseases such as Alzheimer's disease,[7] Down's syndrome,[8] diabetes,[9] and liver cirrhosis.[10] However, the mechanism of the physiological and pathological functions of H_2S still has not been fully elucidated. Hence, the rapid, facile and reliable detection of this small molecule in a living system is crucial to understand its roles in biology and medicine, which has been a research hotspot in recent years.

Optical detection of trace amounts of analytes has received considerable interest because of its simplicity, high sensitivity, and compatibility with real-time monitoring. Fluorescence microscopy is a powerful tool for nondestructive detection of analytes in live cells, tissues and animals.[11−14] Organic fluorophores have been extensively used as bioimaging reagents due to their high absorptivities and emission quantum yields, providing excellent detectability. Recently, a lot of examples of organic fluorophore-based probes have been designed to detect H_2S based on different sensing mechanisms,[15] such as azide reduction,[16−20] quencher (such as Cu^{2+}) removal,[21] and nucleophilic reactions.[22−26] Although a rapid progress has been achieved in last three years, there are still problems to be solved. For example, most reported probes need ultraviolet or visible light as the excitation source, which is harmful to live cells. Moreover, many probes are based on organic π-skeleton and exhibit poor water solubility. Biologically toxic solvents, such as dimethyl sulfoxide (DMSO), tetrahydrofuran (THF), and acetonitrile (CH_3CN), are required to prepare homogeneous solutions for sensing and bioimaging. Furthermore, the biocompability of H_2S probes should be considered in the design of probes for in vivo applications.

Recently, lanthanide-doped upconversation nanoparticles (UCNPs), which convert near-infrared (NIR) radiation to visible light, have received considerable attention for applications in sensing and bioimaging due to their several outstanding features.[27−30] UCNPs offer high photostability and thermal stability. In addition, the NIR excitation source (typically 980 nm) not only offers a substantially higher tissue penetration depth (up to 10 mm) and causes less damage to biological samples than UV excitation source, but also features minimum interference from background autofluorescence by biomolecules in the living systems, resulting in significantly

Received: June 3, 2014
Accepted: July 9, 2014
Published: July 9, 2014

   dx.doi.org/10.1021/am5035158 | ACS Appl. Mater. Interfaces 2014, 6, 11013−11017

improved signal-to-noise ratios. Thus, UCNPs become good candidates for realizing excellent H_2S probes.

In the present study, to solve these problems, we designed a H_2S probe (Figure 1) based on lanthanide-doped upconversion

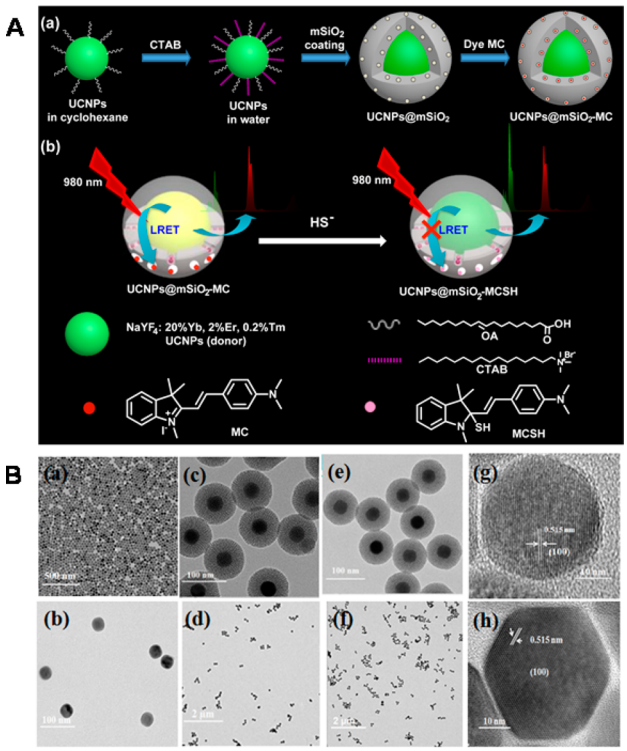

Figure 1. (A-a) Design strategy and synthetic route of nanoprobe UCNPs@SiO_2-MC. (A-b) Sensing mechanism and LRET process of UCNPs@SiO_2-MC toward HS^-. TEM (B-a, B-b) and HRTEM (B-g, B-h) images of OA-UCNPs. (B-c, B-d) TEM images of UCNPs@$mSiO_2$ and(B-e, B-f) UCNPs@$mSiO_2$-MC. (UCNPs = $NaYF_4$: 20% Yb, 2% Er, 0.2% Tm).

nanoparticles. Additionally, mesoporous silica ($mSiO_2$) was involved in the probe because of its fascinating properties, such as large surface area, good water dispersibility, excellent biocompatibility, high stability, and facile surface functionalization. Furthermore, we tried to achieve the ratiometric detection, because compared to intensity-based optical probes whose intensity changes in response to H_2S, ratiometric probes show increased sensitivity and allow the accurate and quantitative measurement of the intracellular H_2S by measuring the ratio changes of the luminescence intensities at two different wavelengths, which can minimize the external environment influences.

Finally, the probe was designed as an organic/inorganic hybrid core−shell structure, where the core is made of upconversion nanocrystals $NaYF_4$: 20% Yb, 2% Er, 0.2% Tm and the shell is $mSiO_2$ containing a merocyanine-based H_2S sensitive dye MC (Figure 1A-a). Upon NIR excitation at 980 nm, efficient luminescence resonance energy transfer (LRET) from the UCNPs to MC occurred (Figure 1A-b), because of the significant spectral overlap of the green upconversion luminescence (UCL) of UCNPs at 514−560 nm and the absorption of MC at 548 nm (ε = 2.56 × 10^4 M^{-1} cm^{-1}) (Figure 2). After the reaction with HS^-, the most stable form of H_2S in the physiological condition, the MC dye was converted to MCSH (Figure 1 and Figure S3 in the Supporting

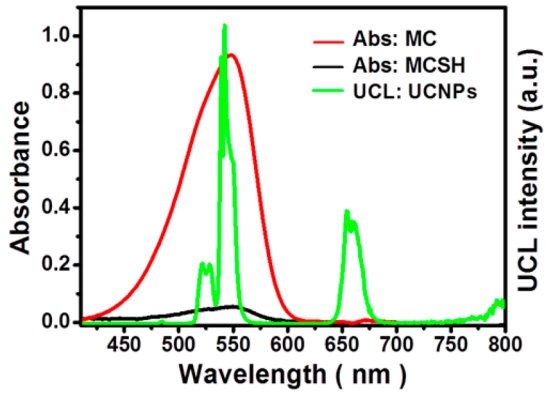

Figure 2. Absorption spectra of MC and MCSH, and UCL spectrum of UCNPs ($NaYF_4$: 20% Yb, 2% Er, 0.2% Tm).

Information),[24] accompanied by a considerable decrease in its absorbance at 548 nm (Figure 2), which reduced the LRET efficiency. Therefore, the green UCL was restored. Thus, using the UCL at 800 nm as an internal standard, the core−shell nanoparticles can be used for ratiometric detection of H_2S with high sensitivity and selectivity.

The preparation of UCNPs@mSiO2-MC is shown in Figure 1A-a and the Supporting Information. First, the core hexagonal NaYF4:20% Yb, 2% Er, 0.2% Tm nanocrystal was prepared by a solvothermal method with oleic acid (OA) as the surface ligand. Next, it was coated with a mesoporous silica shell to form the core−shell structure UCNPs@$mSiO_2$. Then, MC was entrapped into the nanochannels of the $mSiO_2$ shell to yield the nanoprobe UCNPs@$mSiO_2$-MC. The structure of the UCNPs core and core−shell nanoparticles were characterized by transmission electron microscopy (TEM), high-resolution TEM (HRTEM), dynamic light scattering (DLS), energy-dispersive X-ray analysis (EDXA), X-ray powder diffraction (XRD), Fourier transform infrared (FTIR) spectroscopy, and nitrogen adsorption/desorption isotherms.

The TEM images (as shown in Figure 1B-a and B-b) of OA-UCNPs revealed that UCNPs disperse well in cyclohexane and have an average diameter of about 35 nm. As shown in Figure S12 in the Supporting Information, the XRD pattern of OA-UCNPs was indexed to the pure hexagonal phase (JPCDS file number 16−0334) of $NaYF_4$, which was also confirmed by the HRTEM image (Figure 1B-g, h). After being coated with a mesoporous silica shell, the surfactant hexadecyl trimethylammonium bromide (CTAB) was removed completely as it is hazardous by ion exchange in ethanol to produce nanoparticles-(UCNPs@$mSiO_2$). To confirm the removal of CTAB molecules the nanoparticles was investigated by FTIR spectrophotometry. As shown in Figure S6 in the Supporting Information, the peaks at 2927 and 2844 cm^{-1} corresponding to C−H stretching of CTAB molecules disappeared after the ion exchange. The nanoparticle UCNPs@$mSiO_2$ became uniform and monodispersed with an average diameter of about 94 nm (Figure 1B-c and 1B-d), suggesting that the silica layer is about 30 nm in thickness. The wormhole-like disordered mesopores were clearly observed in the silica shells, and the disordered nature of the $mSiO_2$ shell was consistent with the results of small-angle XRD (see Figure S12 in the Supporting Information). The XRD pattern of UCNPs@$mSiO_2$ was shown in Figure S11 in the Supporting Information, and a new peak at 2θ = 22° suggested that amorphous silica was successfully coated on the surface of the UCNPs. The nitrogen

dx.doi.org/10.1021/am5035158 | ACS Appl. Mater. Interfaces 2014, 6, 11013−11017

adsorption and desorption data of the nanoparticles showed typical reversible type IV isotherms for UCNPs@mSiO$_2$ (see Figure S7 in the Supporting Information), which is an important characteristic of mesoporous materials. The specific surface area was obtained from Brunauer–Emmett–Teller (BET) treatment of the isotherm, and the pore volume and pore size were estimated by using the Barrett–Joyner–Halenda (BJH) method. UCNPs@mSiO2 showed a BET surface area of 513 $m^2\ g^{-1}$ and a pore volume of 0.991 $cm^3\ g^{-1}$. The pore size was uniform and a sharp peak located at 2.8 nm in the distribution curve indicated the narrow distribution.

After adsorption of dye MC, the nanoparticles UCNPs@mSiO$_2$-MC can be monodispersed in water (Figure 1B-e, f). The successful adsorption of MC into the nanoparticle surface was also demonstrated by FTIR. As shown in Figure S8 in the Supporting Information, the bands at 1097 cm^{-1} in the FTIR spectra of UCNPs@mSiO$_2$ and UCNPs@mSiO$_2$-MC can be attributed to the characteristic absorption band of Si–O band. In comparison with the FTIR spectrum of UCNPs@mSiO$_2$, new intense band at 1647 cm^{-1} attributed to C=O stretching vibration, can be observed in that of UCNPs@mSiO$_2$-MC. Moreover, the peaks at 1527 and 1572 cm^{-1} can be attributed to the C=C skeleton vibration. The above results have demonstrated that MC is successfully adsorbed in UCNPs@mSiO$_2$.

Based on the absorption spectra of the nanoprobe in solution (1.26 mg/mL), the concentration of the adsorped dye MC was calculated to be 2.28×10^{-5} mol/L. The loading density of MCs after the reaction was approximately 5480 ± 10 molecules per nanoparticle, as determined by UV/vis absorption spectroscopy, corresponding to 7.82 mg of dye MC per gram of nanoprobe. Although dye MC was entrapped into the nanochannels of mSiO$_2$ through physical adsorption, the nanoprobe is stable in H_2O and no evident variation in absorption spectrum was observed in PBS (phosphate buffered saline) solution during the test, indicating that the nanoprobe UCNPs@mSiO$_2$-MC is sufficiently stable for sensing and bioimaging experiments.

The sensing performance of UCNPs@mSiO$_2$-MC was investigated through UV–vis absorption and photoluminescence titrations. As shown in Figure 3a, the nanoprobe exhibits intense absorption bands in the region of 450–600 nm, which was assigned to the charge-transfer transition of the organic dye MC. The addition of HS^- induced significant hypochromicity at 548 nm, indicating the nucleophilic addition reaction between dye MC and HS^-. The reaction reached an equilibrium when 115 μM of HS- were added, accompanied by drastic color change from pink to colorless (see Figure S13 in the Supporting Information). In the photoluminescence titration, the nanoprobe exhibited significant green-UCL enhancement at 514–560 nm upon addition of HS^- (Figure 3b). The intensity of the red UCL at 635–680 nm was also increased slightly and that at 800 nm was unaffected. The ratio I_{540}/I_{800} was used to reflect the concentration of HS^-, which shows a linear increase in the range of 0–115 μM HS^-. The detection limit was estimated to be as low as 0.58 μM, which was lower than that of other merocyanine-based H_2S probe (1.0 μM).[24] Such a low detection limit can be attributed to the ratiometric detection and a low fluorescence background for UCL detection. Additionally, the nanoprobe exhibited selective preference for HS^- over other common inorganic anions including F^-, Cl^-, Br^-, NO_3^-, NO_2^-, and SO_4^- and biological thiols such as cysteine, homocysteine, glutathione, and BSA

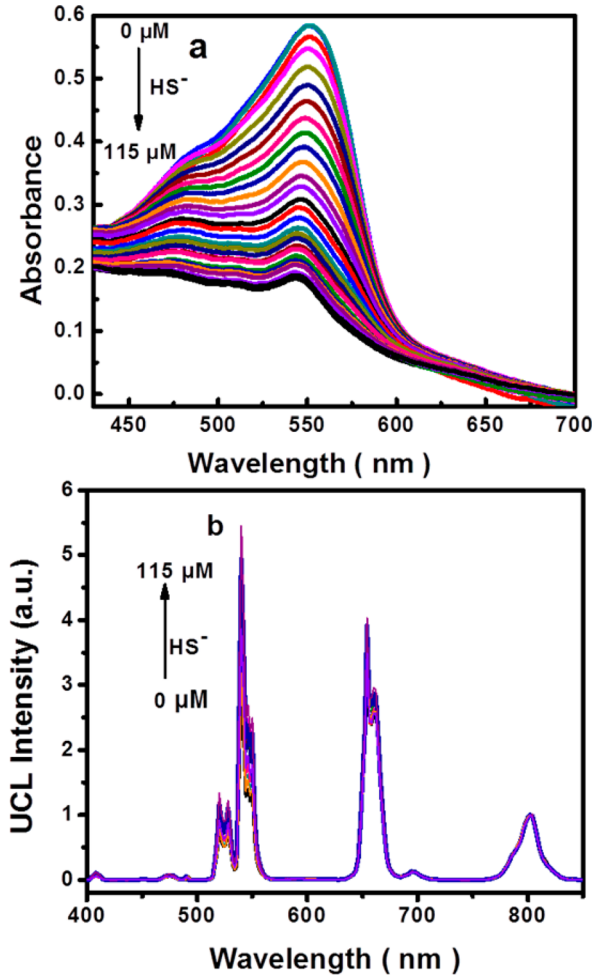

Figure 3. (a) Absorption spectra and (b) UCL spectra of 22.8 μM UCNPs@mSiO$_2$-MC in PBS (pH 7.40) upon addition of HS^-.

(see Figures S13 and S14 in the Supporting Information). These results suggested that UCNPs@mSiO$_2$-MC is suitable for measurement of HS^- in an intracellular environment, where large amounts of inorganic anions and biological thiols exist.

Before cellular applications, the cytotoxicity of UCNPs@mSiO$_2$-MC was investigated by the reduction activity of the methyl thiazolyl tetrazolium (MTT) assay. The viability of untreated cells was assumed to be 100%. Incubation of HeLa cells with 100–600 $\mu g\ mL^{-1}$ UCNPs@mSiO$_2$-MC for 48 h did not revealed evident difference in the cell proliferation (Figure 4j). After incubation with 500 $\mu g\ mL^{-1}$ UCNPs@mSiO$_2$-MC for 48 h, the cellular viability of HeLa cells was higher than 80% even at a high-dose concentration, indicative of low cytotoxicity and good biocompability of the nanoprobe UCNPs@mSiO$_2$-MC. These data indicate that UCNPs@mSiO$_2$-MC can serve as a potential probe for UCL imaging.

Furthermore, considering the sensitive optical response to HS^- and low cytotoxicity, naonoprobe UCNPs@mSiO$_2$-MC was used to image the intracellular HS^- change. The application of UCNPs@mSiO$_2$-MC in bioimaging of intracellular HS^- was carried out via laser-scanning upconversion luminescence microscopy (LSUCLM) experiments. HeLa cells incubated with UCNPs@mSiO$_2$-MC (5 μM) at 37 °C for 1 h showed very weak UCL emission at green channel of 500–555 nm and red channel of 620–670 nm (Figure 4a and 4b). And the ratio (I_{green}/I_{red}) of the emission intensity at green channel

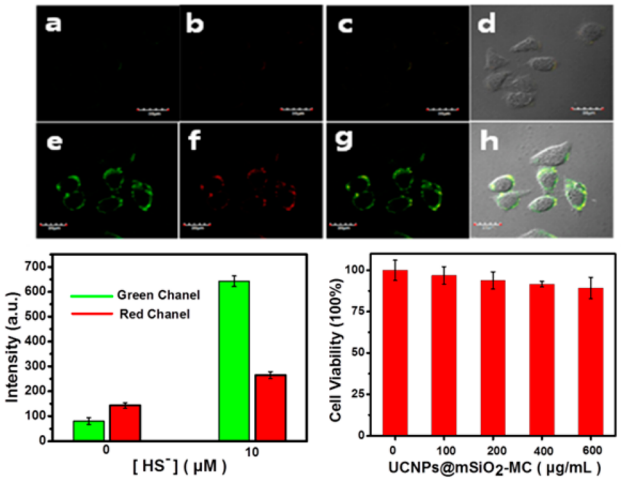

Figure 4. UCL images in (a–d) HeLa cells and (e–h) 10 μM HS^- pretreated HeLa cells incubated with 5 μM UCNPs@$mSiO_2$-MC for 2 h at 37 °C. Emission was collected via (a, e) green UCL channel of 500–555 nm and (b, f) red channel of 620–670 nm. (c, g) Overlay of green and red UCL images. (d, h) Overlay of UCL and brightfield imagings (λ_{ex} = 980 nm). (i) Intensity analysis of green and red UCL collected at the intracellular regions before and after treating with HS^-. (j) In vitro cell viability of HeLa cells incubated with UCNPs@$mSiO_2$-MC with different concentrations (0, 100, 200, 400, and 600 μg/mL) for 48 h at 37 °C.

to that at red channel was measured to be 0.56 (Figure 4i). When the cells were supplemented with 10 μM HS^- in the growth medium for 20 h at 37 °C and then incubated with UCNPs@$mSiO_2$-MC under the same conditions, a significant enhancement of over 8 fold for the green UCL emission and a slight enhancement of about 1.9 fold for the red UCL emission were observed in the intracellular region (Figure 4e and 4f). The ratio of I_{green}/I_{red} was changed to be 2.43 (Figure 4i). Such an evident change of I_{green}/I_{red} before and after treatment of HS^- suggests that UCNPs@$mSiO_2$-MC was suitable for monitoring the change of intracellular HS^- in a ratiometric mode. Brightfield measurements with or without treatment with HS^- confirmed that the cells remained viable throughout the imaging experiments. Overlay of UCL imaging and brightfield images revealed that the UCL signals were localized in the cytosol region (Figure 4h), indicating the subcellular distribution of HS^-.

In summary, a novel core–shell UCL nanoprobe for imaging of intracellular H_2S has been prepared by adsorbing merocyanine into the mesopores of $mSiO_2$ shell of $NaYF_4$: 20% Yb, 2% Er, 0.2% Tm nanocrystals. Utilizing the tunable LRET efficiency induced by the nucleophilic addition reaction between merocyanine and HS^-, the nanoprobe has been used for ratiometric sensing of H_2S with high sensitivity and selectivity. Moreover, this UCL nanoprobe has been used for monitoring H_2S in living cells by means of LSUCLM experiments. To the best of our knowledge, this is the first example of a UCL probe for both sensing and bioimaging of H_2S in the ratiometric mode. The results obtained in this work provide a useful design strategy of novel UCL probes for physiologically relevant species (such as reactive sulfur, nitrogen and oxygen species) in living cells.

■ ASSOCIATED CONTENT

Supporting Information

Additional characterization details. This material is available free of charge via the Internet at http://pubs.acs.org.

■ AUTHOR INFORMATION

Corresponding Authors

*E-mail: iamqzhao@njupt.edu.cn.

*E-mail: wei-huang@njtech.edu.cn.

Notes

The authors declare no competing financial interest.

■ ACKNOWLEDGMENTS

We thank the National Basic Research Program of China (2012CB933301), National Natural Science Foundation of China (61274018, 21174064, and 21171098), the Ministry of Education of China (IRT1148), Program for New Century Excellent Talents in University (NCET-12-0740), Natural Science Foundation of Jiangsu Province of China (BK20130038), Priority Academic Program Development of Jiangsu Higher Education Institutions and the Science Foundation of Nanjing University of Posts and Telecommunications (NY212030) for financial support.

■ REFERENCES

(1) Morita, T.; Perrella, M. A.; Lee, M. E.; Kourembanas, S. Smooth Muscle Cell-Derived Carbon Monoxide is a Regulator of Vascular cGMP. *Proc. Natl. Acad. Sci. U.S.A.* **1995**, *92*, 1475–1479.

(2) Yang, G. D.; Wu, L. Y.; Jiang, B.; Yang, W.; Qi, J. S.; Wang, R. H2S as a Physiologic Vasorelaxant: Hypertension in Mice with Deletion of Cystathionine γ-Lyase. *Science* **2008**, *322*, 587–590.

(3) Lefer, D. J. A New Gaseous Signaling Molecule Emerges: Cardioprotective role of Hydrogen Sulfide. *Proc. Natl. Acad. Sci. U.S.A.* **2007**, *104*, 17907–17908.

(4) Papapetropoulos, A.; Pyriochou, A.; Altaany, Z.; Yang, G.; Marazioti, A.; Szabó, C. Hydrogen Sulfide is an Endogenous Stimulator of Angiogenesis. *Proc. Natl. Acad. Sci. U.S.A.* **2009**, *106*, 21972–21977.

(5) Yang, G.; Wu, L.; Wang, R. Pro-Apoptotic Effect of Endogenous H2S on Human Aorta Smooth Muscle Cells. *FASEB J.* **2006**, *20*, 553–555.

(6) Wallace, J. L.; Caliendo, G.; Santagada, V.; Cirino, G.; Fiorucci, S. Gastrointestinal Safety and Anti-Inflammatory Effects of a Hydrogen Sulfide–Releasing Diclofenac Derivative in the Rat. *Gastroenterology* **2007**, *132*, 261–271.

(7) Eto, K.; Asada, T.; Arima, K.; Makifuchi, T.; Kimura, H. Brain Hydrogen Sulfide is Severely Decreased in Alzheimer's Disease. *Biochem. Biophys. Res. Commun.* **2002**, *293*, 1485–1488.

(8) Kamoun, P.; Belardinelli, M.-C.; Chabli, A.; Lallouchi, K.; Chadefaux-Vekemans, B. Endogenous Hydrogen Sulfide Overproduction in Down Syndrome. *Am. J. Med. Genet., Part A* **2003**, *116*, 310–311.

(9) Yang, W.; Yang, G.; Jia, X.; Wu, L.; Wang, R. Activation of KATP Channels by H2S in Rat insulin-secreting Cells and the Underlying Mechanisms. *J. Physiol.* **2005**, *569*, 519–531.

(10) Fiorucci, S.; Antonelli, E.; Mencarelli, A.; Orlandi, S.; Renga, B.; Morelli, A. The Third Gas: H2S Regulates Perfusion Pressure in Both the Isolated and Perfused Normal Rat Liver and in Cirrhosis. *Hepatology* **2005**, *42*, 539–548.

(11) Yang, Y.; Zhao, Q.; Feng, W.; Li, F. Luminescent Chemodosimeters for Bioimaging. *Chem. Rev.* **2013**, *113*, 192–270.

(12) Kobayashi, H.; Ogawa, M.; Alford, R.; Choyke, P. L.; Urano, Y. New Strategies for Fluorescent Probe Design in Medical Diagnostic Imaging. *Chem. Rev.* **2010**, *110*, 2620–2640.

(13) Zhang, J.; Campbell, R. E.; Ting, A. Y.; Tsien, R. Y. Creating New Fluorescent Probes for Cell Biology. *Nature* **2002**, *3*, 906–918.

(14) Zhao, Q.; Huang, C.; Li, F. Phosphorescent Heavy-Metal Complexes for Bioimaging. *Chem. Soc. Rev.* **2011**, *40*, 2508−2524.
(15) Xuan, W.; Sheng, C.; Cao, Y.; He, W.; Wang, W. Fluorescent Probes for the Detection of Hydrogen Sulfide in Biological Systems. *Angew. Chem., Int. Ed.* **2012**, *51*, 2282−2284.
(16) Lippert, A. R.; New, E. J.; Chang, C. J. Reaction-Based Fluorescent Probes for Selective Imaging of Hydrogen Sulfide in Living Cells. *J. Am. Chem. Soc.* **2011**, *133*, 10078−10080.
(17) Peng, H.; Cheng, Y.; Dai, C.; King, A. L.; Predmore, B. L.; Wang, B. A Fluorescent Probe for Fast and Quantitative Detection of Hydrogen Sulfide in Blood. *Angew. Chem., Int. Ed.* **2011**, *50*, 9672−9675.
(18) Chen, S.; Chen, Z.; Ren, W.; Ai, H. Reaction-Based Genetically Encoded Fluorescent Hydrogen Sulfide Sensors. *J. Am. Chem. Soc.* **2012**, *134*, 9589−9592.
(19) Lin, V. S.; Lipperta, A. R.; Chang, C. J. Cell-trappable Fluorescent Probes for Endogenous Hydrogen Sulfide Signaling and Imaging H2O2-dependent H2S Production. *Proc. Natl. Acad. Sci. U.S.A.* **2013**, *110*, 7131−7135.
(20) Bae, S. K.; Heo, C. H.; Choi, D. J.; Sen, D.; Cho, B. R.; Kim, H. M. A Ratiometric Two-Photon Fluorescent Probe Reveals Reduction in Mitochondrial H2S Production in Parkinson's Disease Gene Knockout Astrocytes. *J. Am. Chem. Soc.* **2013**, *135*, 9915−9923.
(21) Sasakura, K.; Hanaoka, K.; Shibuya, N.; Mikami, Y.; Kimura, Y.; Kimura, H.; Nagano, T. Development of a Highly Selective Fluorescence Probe for Hydrogen Sulfide. *J. Am. Chem. Soc.* **2011**, *133*, 18003−18005.
(22) Liu, C.; Pan, J.; Li, S.; Zhao, Y.; Wu, L. Y.; Berkman, C. E.; Whorton, A. R.; Xian, M. Capture and Visualization of Hydrogen Sulfide by a Fluorescent Probe. *Angew. Chem., Int. Ed.* **2011**, *50*, 10327−10329.
(23) Qian, Y.; Karpus, J.; Kabil, O.; Zhang, S. Y.; Zhu, H. L.; He, C. Selective Fluorescent Probes for Live-cell Monitoring of Sulphide. *Nat. Commun.* **2011**, *2*, 495.
(24) Chen, Y.; Zhu, C.; Yang, Z.; Chen, J.; He, Y.; Guo, Z. A Ratiometric Fluorescent Probe for Rapid Detection of Hydrogen Sulfide in Mitochondria. *Angew. Chem., Int. Ed.* **2013**, *52*, 1688−1691.
(25) Wang, X.; Sun, J.; Zhang, W.; Ma, X.; Lv, J.; Tang, B. A Near-Infrared Ratiometric Fluorescent Probe for Rapid and Highly Sensitive Imaging of Endogenous Hydrogen Sulfide in Living Cells. *Chem. Sci.* **2013**, *4*, 2551−2556.
(26) Wang, J.; Lin, W.; Li, W. Three-Channel Fluorescent Sensing via Organic White Light-Emitting Dyes for Detection of Hydrogen Sulfide in Living Cells. *Biomaterials* **2013**, *34*, 7429−7436.
(27) Wang, F.; Liu, X. G. Recent Advances in The Chemistry of Lanthanide-Doped Upconversion Nanocrystals. *Chem. Soc. Rev.* **2009**, *38*, 976−989.
(28) Fischer, L. H.; Harms, G. S.; Wolfbeis, O. S. Upconverting Nanoparticles for Nanoscale Thermometry. *Angew. Chem., Int. Ed.* **2011**, *50*, 4546−4551.
(29) Zhang, C.; Sun, L. D.; Zhang, Y. W.; Yan, C. H. Rare Earth Upconversion Nanophosphors: Synthesis, Functionalization and Application as Biolabels and Energy Transfer Donors. *J. Rare Earths* **2010**, *28*, 807−819.
(30) Chatterjee, D. K.; Gnanasammandhan, M. K.; Zhang, Y. Small Upconverting Fluorescent Nanoparticles for Biomedical Applications. *Small* **2010**, *6*, 2781−2795.